Ortho-Para-Dependent Pressure Effects Observed in the Near Infrared Band of Acetylene by Dual-Comb Spectroscopy

Kana Iwakuni, Sho Okubo, Koichi M. T. Yamada, Hajime Inaba, Atsushi Onae, Feng-Lei Hong, and Hiroyuki Sasada

Phys. Rev. Lett. **117**, 143902 — Published 29 September 2016

DOI: 10.1103/PhysRevLett.117.143902

Ortho-para dependent pressure effects observed in the near infrared band of acetylene by dual-comb spectroscopy

Kana Iwakuni,[1,2,3] Sho Okubo,[2,3,*] Koichi M. T. Yamada,[4] Hajime Inaba,[2,3] Atsushi Onae,[2,3] Feng-Lei Hong,[2,3,5] and Hiroyuki Sasada[1,3]

[1]*Department of Physics, Faculty of Science and Technology, Keio University, Yokohama 223-8522, Japan*
[2]*National Metrology Institute of Japan (NMIJ), National Institute of Advanced Industrial Science and Technology (AIST), Tsukuba, 305-0045, Japan*
[3]*JST, ERATO, MINOSHIMA Intelligent Optical Synthesizer Project, Tsukuba, 305-8563, Japan*
[4]*Environmental Management Research Institute (EMRI), National Institute of Advanced Industrial Science and Technology (AIST), Tsukuba, 305-8569, Japan*
[5]*Department of Physics, Graduate School of Engineering, Yokohama National University, Yokohama 240-8501, Japan*

(Dated: August 23, 2016)

We demonstrate that dual-comb spectroscopy, which allows one to record broadband spectra with high frequency accuracy in a relatively short time, provides a real advantage for the observation of pressure-broadening and pressure-shift effects. We illustrate this with the $\nu_1 + \nu_3$ vibration band of $^{12}C_2H_2$. We observe transitions from $P(26)$ to $R(29)$, which extend over a 3.8 THz frequency range, at six pressures ranging up to 2654 Pa. Each observed absorption line profile is fitted to a Voigt function yielding pressure-broadening and pressure-shift coefficients for each rotation-vibration transition. The effectiveness of this technique is such that we are able to discern a clear dependence of the pressure-broadening coefficients on the nuclear spin state, i.e. on the ortho or para modification. This information, combined with the pressure shift coefficients, can facilitate a detailed understanding of the mechanism of molecular collisions.

Spectroscopy has a long history: from Fraunhofer's discovery of dark lines in the solar spectrum to recent detailed studies of the interaction between materials and radiation. It was fundamental in the invention of lasers, which have in turn further advanced the frontier of spectroscopy itself. Development of the optical frequency-comb based on mode-locked laser has dramatically simplified precise optical frequency measurements in the visible and near-infrared regions [1–3]. The optical frequency comb has also been used as a broadband light source for Fourier transform spectroscopy [4–6]. In particular dual-comb spectroscopy is useful for quickly obtaining broad spectra while still maintaining high spectral resolution and high frequency accuracy [7, 8]. These features are suitable for comprehensive investigation of pressure effects on rotation-vibration transitions across an entire molecular vibrational band.

The $\nu_1+\nu_3$ band of acetylene has been repeatedly studied spectroscopically for application to optical communications. The center frequencies of most of the rotation-vibration lines of this band have been determined with an uncertainty of about 15 kHz in sub-Doppler resolution spectroscopy [9] and of about 2 kHz using optical frequency combs as a frequency ruler [10]. Dual-comb spectroscopy has also been applied to this band in Doppler-limited resolution [8, 11, 12] and the line center frequencies found there are in excellent agreement with those determined by sub-Doppler resolution spectroscopy [10]. Pressure effects on the spectral lines of this band due to collisions between the acetylene molecules (self-pressure effects) have been investigated using continuous wave (CW) lasers [13–16]. However, to the best of our knowledge, no previous work has used optical frequency combs as a light source in the study of pressure effects. With dual-comb spectroscopy, pressure effects of tens of lines can be investigated under common experimental conditions such as the gas pressure, the temperature, the laser power, and the optical alignment.

When molecules contain identical nuclei the statistical weights of the molecular levels depend on the molecular symmetry and the spin of the identical nuclei [17]. For the ground vibrational state of $^{12}C_2H_2$, as for H_2, those rotational levels with odd angular momentum quantum number, J, are called the *ortho* modification and have a nuclear spin weight of three, while those with even angular momentum quantum number are called the *para* modification and have weight one. In the absence of nuclear spin interactions only ortho-ortho and para-para transitions are allowed in general.

In this work we find that, although the overall trend of the pressure broadening coefficient varies rather smoothly with J, there is a distinct alternation of its value around this trend. We find that transitions involving ortho levels tend to have larger broadening coefficients than the transitions involving adjacent para rotational levels, that is, adjacent values of J. For example the pressure-broadening of the $R(7)$ transition is 12 % larger than that of the $R(8)$ transition. To our knowledge, ortho/para dependent pressure broadening has not previously been observed.

Figure 1 shows an overview of the experimental setup. Details are described elsewhere [12]. The two femtosec-

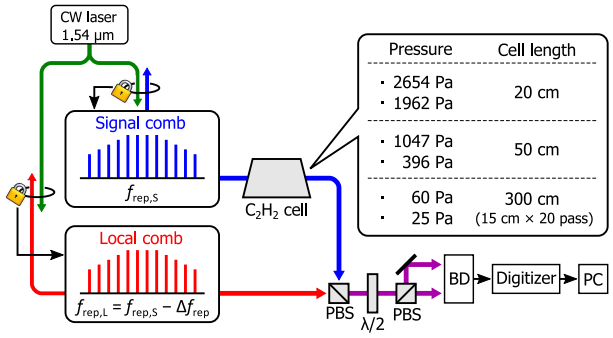

FIG. 1. Setup of present dual-comb spectrometer: PBS (polarization-dependent beam splitter), $\lambda/2$ (half-wave plate), BD (balanced detector).

ond Er-doped fiber lasers each generate a separate frequency comb. One of these is led through the sample chamber and is therefore called the signal comb. Light from the other comb serves as a local oscillator (local comb). These two combs are set up with very slightly different repetition rates $f_{\mathrm{rep,S}}$ and $f_{\mathrm{rep,L}} = f_{\mathrm{rep,S}} - \Delta f_{\mathrm{rep}}$. An entire interferogram is recorded in the time $(\Delta f_{\mathrm{rep}})^{-1}$, which is typically of the order of 10 ms, considerably shorter than in conventional FTIR. The spectrum is then obtained by Fourier transformation of the interferogram. In this study the repetition rate of the signal comb $f_{\mathrm{rep,S}}$ is set to 48 MHz. Each of the two comb modes and each carrier envelope offset frequency are respectively phase-locked to a common 1.54-μm CW laser and RF synthesizer. These two phase locks reduce the relative linewidth of the two combs to less than 1 Hz. This enables us to accumulate many data runs to enhance sensitivity. Furthermore, we can decrease the difference between the repetition rates of the two optical frequency combs, Δf_{rep}, and thus increase the Nyquist-condition limited spectral span to enable us to observe the entire $\nu_1 + \nu_3$ vibration band of $^{12}C_2H_2$ in one shot.

The sample absorption cell is inserted in the optical path of the signal comb. A 20-cm long cell is used for the measurements with the sample at pressures of 2654 Pa and 1962 Pa, a 50-cm long cell for those at 1047 Pa and 396 Pa, and a White cell (15 cm long, 10 round-trips) for those at 60 Pa and 25 Pa. The sample pressure is measured with a PZT gauge, with a guaranteed accuracy of $\pm 1\%$ for pressures higher than 133 Pa. For sample pressures less than 133 Pa, the PZT gauge is calibrated with air using an absolute pressure gauge.

The value of Δf_{rep} is usually set at 45 Hz or, for the pressure of 60 Pa, 33 Hz. Interferograms are averaged 10000 times using the coherent averaging technique [18], and the total measurement time is 222 s for $\Delta f_{\mathrm{rep}} = 45$ Hz and 303 s for $\Delta f_{\mathrm{rep}} = 33$ Hz. The environmental temperature of the laboratory including the sample cells is kept at $T_{\mathrm{room}} = 22.5 \pm 0.5$°C.

According to Lambert-Beer's law, the power transmitted through the absorption cell is,

$$I(\nu) = I_0(\nu)\exp[-\sigma V(\nu, \nu_0)], \tag{1}$$

where $I_0(\nu)$ is the incident power of radiation, ν is the optical frequency, ν_0 is the center frequency of an absorption line, σ is the intensity factor, and $V(\nu, \nu_0)$ is the Voigt function [19];

$$V(\nu, \nu_0) = \frac{\Delta_{\mathrm{L}}}{\pi^{\frac{3}{2}}\Gamma_{\mathrm{G}}} \int_{-\infty}^{+\infty} \frac{\exp[-(\nu - \nu_1)^2/\Gamma_{\mathrm{G}}^2]}{(\nu_1 - \nu_0)^2 + \Delta_{\mathrm{L}}^2} d\nu_1. \tag{2}$$

Here, Δ_{L} and Γ_{G} are Lorentzian width (half-width at half maximum) and Doppler width (half width at $1/e$ maximum), respectively. Since $I_0(\nu)$ cannot be measured directly, we instead use $I_{\mathrm{ref}}(\nu)$, the detected power of radiation transmitted when the cell is evacuated. The measured spectral transmittance is then calculated as the ratio of the measured transmitted power, $I(\nu)$, and $I_{\mathrm{ref}}(\nu)$, that is as $I(\nu)/I_{\mathrm{ref}}(\nu)$. Figure 2(a) shows the transmittance of the $^{12}C_2H_2$ lines around 197.2 THz with a sample pressure of 60 Pa. The frequency axis of the spectrum is scaled with the absolute frequency, and the frequency uncertainty of the spectrum is less than 20 kHz.

Figure 2(b) shows the normalized absorbance of the $R(9)$ transition for the six different sample pressures. The Lorentzian width, which increases in proportional to the sample pressure, is appreciable in comparison to the Doppler width at the high pressure points. The

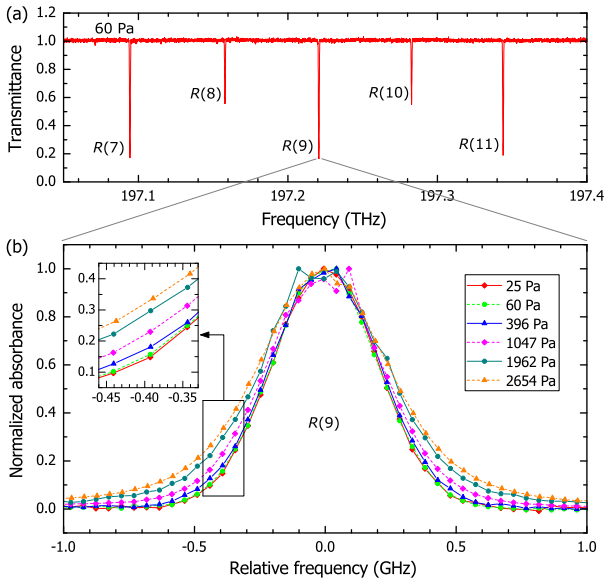

FIG. 2. (a) Transmittance spectrum around 197.2 THz with sample pressure of 60 Pa. (b) Normalized absorbance of the $R(9)$ transition with different sample pressures. The horizontal axis is the frequency relative to the transition frequency measured with sub-Doppler resolution spectroscopy [10]. The Doppler width (half-width at half maximum) for this transition is 238 MHz. Because of the large absorbance, small noise near the line center is enhanced in this type of plot.

center frequency, Lorentzian width, and intensity factor are determined by fitting the measured transmittance, $I(\nu)/I_{\rm ref}(\nu)$, to the model function of $(a_0 + a_1\nu)\exp[-\sigma V(\nu,\nu_0)]$. Each line in the present study is fitted over the range $\nu_0 - 2$ GHz to $\nu_0 + 2$ GHz. Here the Gaussian width in the Voigt function is fixed for each line at the theoretical value of the Doppler width at the laboratory temperature of 22.5 ± 0.5 °C. The factor of $(a_0 + a_1\nu)$ is inserted as a simple linear model to correct for the difference between $I_{\rm ref}(\nu)$ and $I_0(\nu)$ in the 4 GHz frequency range of the fit.

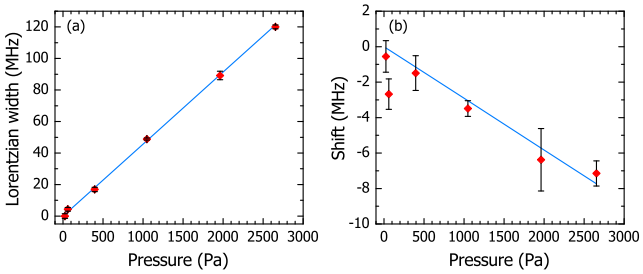

FIG. 3. The pressure effects of the $R(9)$ transition plotted as a function of the sample pressure. (a) Lorentzian width. (b) Line center shift.

The Lorentzian width $\Delta_{\rm L}$ of the $R(9)$ transition is shown as a function of the sample pressure, P, in Fig. 3(a). Neither natural nor transit-time broadenings are considered because the magnitudes of these are less than our measurement uncertainty. The pressure broadening coefficient, b, is determined for each transition by a weighted least-squares fitting of the Lorentzian widths to the linear expression, $\Delta_{\rm L} = bP$. This same analysis is carried out for all transitions from $P(26)$ to $R(29)$, which range in frequency from 194.5 to 198.3 THz. The resulting pressure broadening coefficients for each rotation-vibration transition are shown in Fig. 4(a) by circles (red online) for ortho transitions and diamonds (blue online) for para transitions. Here $m = J'' + 1$ for the R-branch transitions, and $m = -J''$ for the P-branch transitions, where J'' is the rotation angular momentum quantum number of the lower level of the transition. Although the typical uncertainty is about 0.5 kHz/Pa, the pressure broadening coefficients for some transitions have larger uncertainties due to poor signal-to-noise ratio or overlap with hot-band transitions or transitions of isotopologues. In Fig. 4(a) the R-branch transitions ($m > 0$) exhibit a clear zigzag structure, indicating an ortho/para dependence of the pressure broadening. For the P-branch transitions ($m < 0$) this is less evident due to the lower signal-to-noise ratio.

The pressure-broadening coefficients could be modeled by the empirical expression used for the same $\nu_1 + \nu_3$ transition in $^{13}C_2H_2$ by Kusaba and Henningsen [20],

$$b(m) = f_0(m), \tag{3}$$

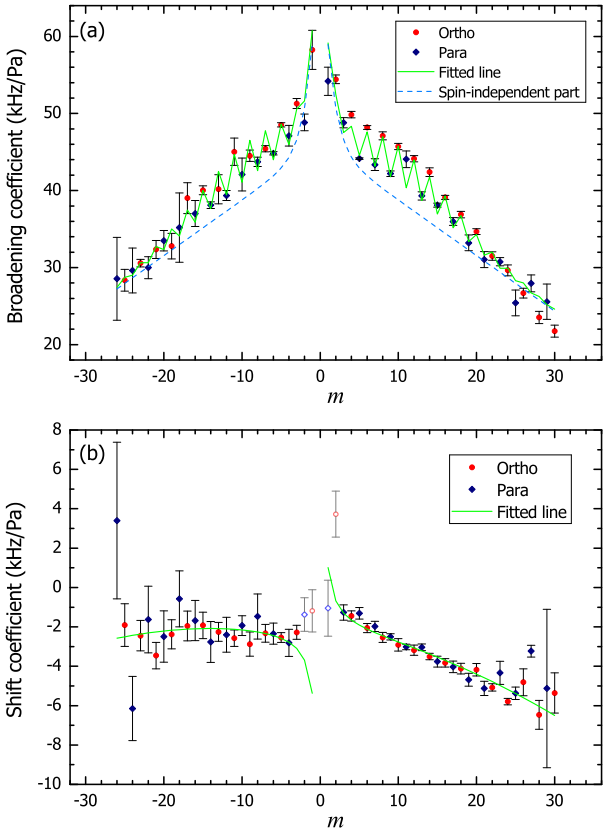

FIG. 4. Pressure coefficients plotted as a function of m, where m is $J'' + 1$ for the R-branch transitions and $-J''$ for the P-branch transitions. (a) Pressure broadening coefficient. Spin independent curve is from Eq. (4) with parameters of $b_1 = 46.0(6)$ kHz/Pa, $b_2 = -0.72(3)$ kHz/Pa, $b_3 = 31(10)$ kHz/Pa, and $b_4 = 0.81(18)$. Fitted line contains spin-dependent part of Eq. (5) with $c_1 = 0.205(14)$ kHz/Pa. The assumed Boltzmann distribution in Eq. (6) has peaks at $m = -9$ and $+10$. (b) Pressure shift coefficient. Fitted line is from Eq. (7) with parameters of $d_{-1} = 3.3(9)$ kHz/Pa, $d_0 = -2.17(12)$ kHz/Pa, $d_1 = -0.063(11)$ kHz/Pa, and $d_2 = -0.0028(5)$ kHz/Pa.

where,

$$f_0(m) = b_1 + b_2|m| + b_3\exp[-b_4|m|]. \tag{4}$$

However, this model cannot describe the ortho/para alternation seen in Fig. 4(a). To model the observed ortho/para alternation we introduce a second term to Eq. (3),

$$b(m) = f_0(m) + f_1(m). \tag{5}$$

The spin dependence of the pressure broadening is not caused by the magnetic intermolecular interaction because it is much smaller than the electric one. Instead, we attribute the difference between the ortho and para broadening to their different spin weight in the Boltzmann population of the rotational level of the *perturber*,

which collides with the *absorber* illuminated with the resonant radiation and gives rise to the "rotational resonance" [21–23]. This effect is taken into consideration by taking the new term as,

$$f_1(m) = c_1(2J'' + 1)g_I \exp[-hBJ''(J'' + 1)/(k_B T)], \quad (6)$$

where c_1 is an overall scaling factor. Other than the factor c_1, $f_1(m)$ only depends on J''(the rotational quantum number associated with m). Here h is Planck's constant, and k_B is the Boltzmann constant. The nuclear spin weight is denoted by g_I. The rotational constant of the ground state, B, is 35.274974274 GHz [10], and the sample gas temperature is assumed to be 296 K.

The five parameters, b_1, b_2, b_3, b_4 of $f_0(m)$ and c_1 of $f_1(m)$, are obtained by a weighted least-squares fitting of Eq. (5) to the observed broadening coefficients. The parameters determined in the fitting are presented in the caption of Fig. 4(a) together with the expected uncertainties, in parentheses, given in units of the last digit. The fitted function is shown by the upper (jagged) curve in Fig. 4(a) and can be seen to agree very well with the experimental pressure-broadening coefficients, not only reproducing the general trend of the broadening coefficients as a function of angular momentum quantum number, but also reproducing the alternation seen in the experimental results, even including the decrease of the magnitude of this alternation at higher J'' levels (higher values of $|m|$).

Equation (5), incorporating the $f_1(m)$ term defined in Eq. (6), thus provides a relevant model for the observed ortho/para dependent pressure broadening. The collision-induced transitions are subject to a certain selection rule determined by a type of the intermolecular interaction. They mainly occur between the molecules of the same nuclear spin modification because the dominant intermolecular interaction does not change the nuclear spin state. Among them, specific collisions, in which the *absorber* and *perturber* exchange the rotational quanta, efficiently contribute to the spectral broadenings. Such effect is often called as the "rotational resonance" [21–23]. In the case of $^{12}C_2H_2$, the electric quadrupole-quadrupole interaction is dominant, and the *absorbers* in the J''-rotational level are thereby in "rotational resonance" with the *perturbers* in the $J'' \pm 2$-rotational levels. Therefore, $f_1(m)$ contains the number of *absorbers* which are approximately proportional to the number of the *perturbers* in "rotational resonance" with the *absorbers*. The differing populations of the collision partners because of their different spin statistical weights, g_I, then lead to an ortho/para dependence of the broadening, as described by the $f_1(m)$ term in Eq. (6).

The self-pressure-broadening coefficients are generally expressed, similarly to Eq. (5), as a sum of the non-rotational-resonant and rotational-resonant terms. In the case of HCN, because the second term is larger than the first term, the self-pressure-broadening coefficients of the rotational levels behave in a similar manner as the rotational population [24, 25]. In the present case of $^{12}C_2H_2$, the two terms in Eq. (5) are separately determined from the measurement because of the different spin statistical weights although the second term is smaller than the first term. It provides usually inaccessible information of intermolecular interactions.

As far as we are aware ortho/para dependence has not previously been observed, even though several other works have investigated self-broadening. This includes Refs. [13, 20, 26, 27] as well as other references therein. In the work of Kusaba and Henningsen [20], the pressure broadening coefficients of the $\nu_1+\nu_3$ band of $^{13}C_2H_2$ were also measured for each rotation-vibration line. Their results are consistent with the present values within their 4–6 % uncertainty limit. The ortho/para ratio in $^{13}C_2H_2$ is a less favourable 5:3 ratio compared to the 3:1 ratio in $^{12}C_2H_2$. For instance, the large difference of the pressure broadening coefficients are observed to be 4.9 kHz/Pa between the $R(7)$ and the $R(8)$ transitions of $^{12}C_2H_2$. If our expression in Eq. (6) is valid, we expect the difference of the pressure broadening coefficients between the $R(7)$ and the $R(8)$ transitions of $^{13}C_2H_2$ to be less than the 2.7 kHz/Pa. This value is comparable with their measurement uncertainty and is therefore consistent with their non-observation of ortho/para dependence.

The pressure dependence of the line center frequencies is also observed and is shown for six sample pressures for the $R(9)$ transition in Fig. 3(b). We take the frequency deviations from the sub-Doppler resolution measurement [10] as the line shifts, which was performed over a pressure range of 1 to 4 Pa. The pressure shift coefficients, Δ, for the $P(26)$ to $R(29)$ transitions data are then obtained by a weighted least-squares fitting of the observed shifts to a simple linear function of the pressure. This figure shows clearly that the pressure-shift coefficients are one order of magnitude smaller than the pressure-broadening coefficients. These coefficients are determined with a typical uncertainty of 0.4 kHz/Pa. Figure 4(b) shows the pressure-shift coefficients as a function of m, with circles (red online) and diamonds (blue online) used for the ortho and para transitions, respectively. These coefficients are then fitted to an empirical polynomial function of m,

$$\Delta(m) = d_{-1}m^{-1} + d_0 + d_1 m + d_2 m^2. \quad (7)$$

Here we add the term proportional to m^{-1} because impact theory predicts a gap in the pressure shift between the $P(1)$ and $R(0)$ transitions [22]. The fitted parameters are presented in the caption of Fig. 4(b), with the expected uncertainties, in parentheses, given in units of the last digit. Figure 4(b) is consistent with Fig. 9 of Ref. [20], although the gap was barely observed there. The curve (green online) in Fig. 4(b) represents the fitted function. The parameter d_{-1} is statistically determined even though the data for the transitions with $m = -2$, -1, 1, and 2 are not included in the fitting because their

line-center positions are not well determined due to overlapping lines and/or poor signal-to-noise ratio. Those points are therefore shown with fainter symbols in Fig. 4(b).

The m-dependence of the pressure shift coefficients has different slopes for the P- and R-branch transitions. No clear ortho/para dependence is evident in these results. Figures 3(a) and 3(b) indicate that the pressure shift is one order of magnitude smaller than the pressure broadening. Therefore, if the spin modification effect is of the same relative magnitude as for the pressure broadening, higher precision would be required to observe any ortho/para dependence of the pressure-shift coefficients.

There have been two conventional methods for determining spectral line parameters such as the center frequency, the peak intensity, and the line width. One is Michelson-type FTIR which uses a black-body radiation-source, and is the current state-of-the-art. The other is CW laser spectroscopy. The former has a wide spectral range, but is less sensitive. In contrast the latter gives faithful line shapes with high sensitivity. However with this technique the spectral lines are recorded one-by-one, taking considerable time during which experimental conditions can change. Furthermore, the tunable range of the CW laser is usually too narrow to record an entire vibrational band. Here we have verified that a third method, dual-comb spectroscopy, has advantages over both conventional methods in accuracy, sensitivity, short data acquisition time, spectral coverage, and, compared to CW laser spectroscopy, greatly improved line-to-line consistency due to the simultaneous nature of Fourier spectroscopy.

In summary, we have demonstrated that dual-comb spectroscopy is a powerful tool to carry out broadband studies with high precision in a short time. It allows us to determine the pressure-broadening and pressure-shift coefficients of the entire $\nu_1+\nu_3$ band of $^{12}C_2H_2$. In the subsequent analysis we identified a hitherto unobserved ortho/para dependence of this pressure-broadening. These surprising results provide data for further understanding of the mechanism of molecular collisions.

We thank Prof. Stephen Ross for his assistance in the preparation of the manuscript. We appreciate Prof. Kevin Lehmann giving us valuable comments.

* sho-ookubo@aist.go.jp

[1] T. Udem, J. Reichert, R. Holzwarth, and T. W. Hänsch, Phy. Rev. Lett. **82**, 3568 (1999).
[2] D. J. Jones, S. A. Diddams, J. K. Ranka, A. Stentz, R. S. Windeler, J. L. Hall, and S. T. Cundiff, Science **288**, 635 (2000).
[3] S. A. Diddams, D. J. Jones, J. Ye, S. T. Cundiff, J. L. Hall, J. K. Ranka, R. S. Windeler, R. Holzwarth, T. Udem, and T. W. Hänsch, Phys. Rev. Lett. **84**, 5102 (2000).
[4] R. M. Godun, P. B. R. Nisbet-Jones, J. M. Jones, S. A. King, L. A. M. Johnson, H. S. Margolis, K. Szymaniec, S. N. Lea, K. Bongs, and P. Gill, Phys. Rev. Lett. **113**, 210801 (2014).
[5] M. J. Thorpe, K. D. Moll, R. J. Jones, B. Safdi, and J. Ye, Science **311**, 1595 (2006).
[6] S. A. Diddams, L. Hollberg, and V. Mbele, Nature **445**, 627 (2007).
[7] F. Keilmann, G. Gohle, and R. Holzwarth, Opt. Lett. **29**, 1542 (2004).
[8] I. Coddington, W. C. Swann, and N. R. Newbury, Phys. Rev. Lett. **100**, 013902 (2008).
[9] K. Nakagawa, M. de Labachelerie, Y. Awaji, and M. Kourogi, J. Opt. Soc. Am. B **13**, 2708 (1996).
[10] A. A. Madej, A. J. Alcock, A. Czajkowski, J. E. Bernard, and S. Chepurov, J. Opt. Soc. Am. B **23**, 2200 (2006).
[11] A. M. Zolot, F. R. Giorgetta, E. Baumann, J. W. Nicholson, W. C. Swann, I. Coddington, and N. R. Newbury, Opt. Lett. **37**, 638 (2012).
[12] S. Okubo, K. Iwakuni, H. Inaba, K. Hosaka, A. Onae, H. Sasada, and F.-L. Hong, Appl. Phys. Express **8**, 082402 (2015).
[13] W. C. Swann and S. L. Gilbert, J. Opt. Soc. Am. B **17**, 1263 (2000).
[14] A. Nadezhdinskii and Y. Ponurovskii, Spectrochim. Acta, Part A **66**, 807 (2007).
[15] C. McRaven, M. Cich, G. Lopez, T. J. Sears, D. Hurtmans, and A. Mantz, J. Mol. Spectrosc. **266**, 43 (2011).
[16] M. Cich, C. McRaven, G. Lopez, T. Sears, D. Hurtmans, and A. Mantz, Appl. Phys. B **109**, 373 (2012).
[17] L. Landau and E. Lifshits, *Quantum Mechanics: Non-relativistic Theory* (Butterworth-Heinemann, 1977), for example.
[18] I. Coddington, W. C. Swann, and N. R. Newbury, Opt. Lett. **34**, 2153 (2009).
[19] K. M. T. Yamada, A. Onae, F.-L. Hong, H. Inaba, and T. Shimizu, C. R. Phys. **10**, 907 (2009).
[20] M. Kusaba and J. Henningsen, J. Mol. Spectrosc. **209**, 216 (2001).
[21] P. W. Anderson, Phys. Rev. **76**, 647 (1949).
[22] C. H. Townes and A. L. Schawlow, *Microwave Spectroscopy* (Dover Publication Inc., 1955).
[23] T. Oka (Academic Press, 1974), vol. 9 of *Advances in Atomic and Molecular Physics*, pp. 127–206.
[24] A. M. Smith, K. K. Lehmann, and W. Klemperer, J. Chem. Phys. **85**, 4958 (1986).
[25] V. M. Devi, D. C. Benner, M. A. H. Smith, C. P. Rinsland, S. W. Sharpe, and R. L. Sams, J. Quant. Spectrosc. Radiat. Transfer **82**, 319 (2003).
[26] J. S. Li, G. Durry, J. Cousin, L. Joly, B. Parvitte, and V. Zeninari, J. Quant. Spectrosc. Radiat. Transfer **111**, 2332 (2010).
[27] D. Jacquemart, J.-Y. Mandin, V. Dana, L. Régalia-Jarlot, X. Thomas, and P. Von der Heyden, J. Quant. Spectrosc. Radiat. Transfer **75**, 397 (2002).